systems

MDPI

Article

Offset Optimization Model for Signalized Intersections Considering the Optimal Location Planning of Bus Stops

Wei Wu [1,2], Xiaoyu Luo [1] and Baiying Shi [3,*]

[1] School of Traffic and Transportation Engineering, Changsha University of Science and Technology, Changsha 410004, China; jiaotongweiwu@csust.edu.cn (W.W.); lxy@stu.csust.edu.cn (X.L.)
[2] College of Traffic and Transportation, Chongqing Jiaotong University, Chongqing 400074, China
[3] School of Traffic Engineering, Shandong Jianzhu University, Jinan 250101, China
* Correspondence: shibaiying@sdjzu.edu.cn; Tel.: +86-186-1526-1373

Abstract: Existing offset optimization methods for signalized intersections are mainly focused on regular traffic flow, which cannot accommodate cars and public transit (e.g., Bus Rapid Transit (BRT)) simultaneously. This study proposes a delay prediction model to formulate the signal delay of BRT at intersections. The relation among the green wave bandwidth, signal timing plans, speed of the BRT vehicles, distance between the intersections, and the offset is also modeled. A combinatorial optimization model is then established, which takes the location planning of BRT stops and the offset of intersections at both directions along the artery as the decision variables. The proposed model is programmed with Mathematical Programming Language (AMPL) and solved efficiently by the Gurobi solver. The proposed optimization method is compared with seven different methods. The results show that the average BRT travel time is reduced by at least 19% and the green wave bandwidth is increased by around 30.2%. The importance of considering location planning of BRT stops when optimizing the offset is thereby verified.

Keywords: bus stop location; offset optimization; BRT; signalized intersection; mathematical programming

Citation: Wu, W.; Luo, X.; Shi, B. Offset Optimization Model for Signalized Intersections Considering the Optimal Location Planning of Bus Stops. *Systems* **2023**, *11*, 366. https://doi.org/10.3390/systems11070366

Academic Editor: Ed Pohl

Received: 31 May 2023
Revised: 12 July 2023
Accepted: 14 July 2023
Published: 18 July 2023

1. Introduction

Urban traffic congestion has become a serious problem in recent years [1–3], which has resulted in extra carbon emissions, energy consumption [4], and travel time [5]. In 2019, urban Americans experienced an excess of 36 million tons of greenhouse gas emissions and 3.5 billion gallons of fuel consumption because of traffic congestion. Furthermore, travel delay increased to 8.7 billion hours, and an extra 22 million USD of total cost (delay time and wasted fuel by all vehicles) were consumed in 2019 compared to 2015 [6]. Therefore, in order to facilitate the urban development and city sustainability, congestion alleviation and prevention have become urgent tasks [7]. However, the growth rate of road construction can never meet the requirements of traffic demand. In recent years, car ownership has steadily increased, and car travel accounts for about 70% of all urban road traffic modes. However, compared to car travel mode, public transportation offers significant advantages in terms of capacity, road area occupancy, energy consumption, and carbon emissions. Specifically, compared to cars, public transportation has approximately 15 times the capacity and occupies only 1/10 of the per capita road area. Furthermore, per capita energy consumption per 100 km traveled by buses is approximately 8.4% that of cars, and carbon emissions per 10,000 km is about 1/7 that of cars.

Therefore, developing and prioritizing public transportation is vital and may be the only efficient method to reduce urban congestion [8], carbon emissions, and energy consumption. One of the most important modes of public transportation is Bus Rapid Transit (BRT), which has been introduced in many cities due to its characteristics of large capacity, exclusive lanes, exclusive stops, and rapid transit. During BRT operations on an

urban artery, traffic delays mainly come from signal delays at the intersections. However, most existing signal timing models of green waves on the artery focus only on the traffic flow of cars. As BRT vehicles need to stop at the stops for passengers to get on and off, there is a longer travel time for BRT vehicles between intersections. The signal coordination control models for cars are difficult to adapt to BRT, and this increases signal delays for the BRT. Accordingly, it is essential to study the signal timing model considering the optimal location planning of BRT stops.

In recent years, scholars have conducted extensive studies on the location planning of bus stops [9], mainly bus stop location optimization [10–16] and stop-spacing optimization [17–21].

In terms of bus stop location optimization, the impact of setting bus stops at the entrance or exit lanes of intersections on bus delays has been analyzed by Cvitanic et al. [10] and Diab et al. [11], who evaluated the impact of bus stop location on bus stop time. Cui et al. [12] constructed a multi-objective optimization model to distribute bus stop locations based on the shortest total walk distance of passengers and the minimum delay time of cars and the travel time of buses. Other scholars have associated bus-stop location optimization with vehicle delay [13,14]. For example, Furth et al. [13] analyzed the influence of bus delays at stops of intersections by considering factors such as deceleration, acceleration, and queuing of buses at the stop. Tirachini et al. [14] analyzed the interaction among the scale of bus stops, bus speed, spacing, and delay. Furthermore, many studies have studied the impacts of the location planning of bus stops on the travel time [15,16]. As larger stop-coverage areas (low density of bus stops) imply longer walking times and shorter bus travel times (fewer stops, less stopping time), a trade-off between them should be made. For example, Shatnawi et al. [16] proposed a bus stop optimization model to shorten the travel time of a bus on the artery by reducing redundant bus stops based on the geographic information system and particle swarm optimization.

In terms of bus stop spacing optimization, previous studies have mainly optimized bus stop spacing considering bus accessibility [17], bus passengers' travel time [18], and bus operation efficiency [19]. For example, Cheng et al. [20] constructed a bi-level objective optimization model of spacing at BRT stops considering the benefits to passengers and bus companies. They revealed the relationship between the location of BRT stops and the service coverage. Chien et al. [18] took the total cost of bus operators and passengers as the objective, and then the number and the location of bus stops are optimized to improve the accessibility of bus services. Ibeas et al. [21] optimized bus stop spacing to minimize the social cost of the transportation system. The above studies on bus stop location optimization and bus stop spacing optimization have led to many useful discoveries, but optimizing bus stop location planning by considering signal timing plans along the artery remains a challenge.

With respect to traffic signal timing along the artery, scholars have conducted extensive research on the coordination control between intersections [22–29], and the offset optimization has always been the focus of research on arterial coordination control [26,27]. In some existing offset optimization methods, traffic flow is modeled as sinusoids and solved via convex semidefinite relaxation [30–32]. However, most of the research uses the space–time trajectory of cars to optimize the offset. For example, Wang et al. [33] constructed an offset optimization model based on the space–time trajectory. The effects of initial queue length, number of arriving vehicles, intersection spacing, and traffic flow composition on offset are analyzed. Nevertheless, most of the offset optimization models are focused on cars and cannot adapt to BRT or other public transit operation. The space-time trajectory of BRT vehicles on the artery are quite different from those of cars, so finding ways to accommodate the traffic flow of cars with BRT vehicles when optimizing offsets needs further study.

Overall, it can be said that the current literature in this area has the following research gaps: (i) studies on the location planning of bus stops considering signal timing plans of multiple intersections on the artery are of limited scope; (ii) most of the existing signal coordination control models along the artery are focused mainly on the flow of cars; and (iii) there are a lack of offset optimization models that consider the location planning of

bus stops, which makes the coordination control method along the artery difficult to apply to buses.

Research assumptions of this paper include: (i) the dwell time of BRT vehicles at the stop is given as parameters; (ii) a bus stop is located at the upstream or at the downstream of each intersection along the arterial; and (iii) the fixed signal timing program is utilized at each intersection. In this paper, the effects of setting BRT stops upstream or downstream of the intersections on the signal delay of BRT are analyzed first, and then a delay prediction model is established. An optimization model of the intersection offset considering the location planning of BRT stops is then proposed considering the green wave bandwidth of cars, the signal timing of intersections, the speed of the BRT vehicles along the artery, and the distance between intersections. In particular, the location planning of BRT stops and the offsets along the multiple intersections for both directions of the artery are optimized simultaneously.

2. Optimization Model

The location planning of BRT stops at intersections can be divided into upstream and downstream stops (stops that are located at the upstream and downstream of the intersection, respectively), as shown in Figure 1, and their effects are very different, as buses can stop once or twice close to the intersection [34]. For intersection i, considering the location planning of the BRT stops at both directions along an artery, there are four possible configurations (schemes), as shown in Figure 1. If there are n intersections on the urban artery, there are 4^n kinds of combining schemes for location planning of BRT stops. In the coordinated control scenario, the location planning of stops and signal control parameters at the upstream intersection will affect the traffic condition of BRT vehicles at the downstream intersection.

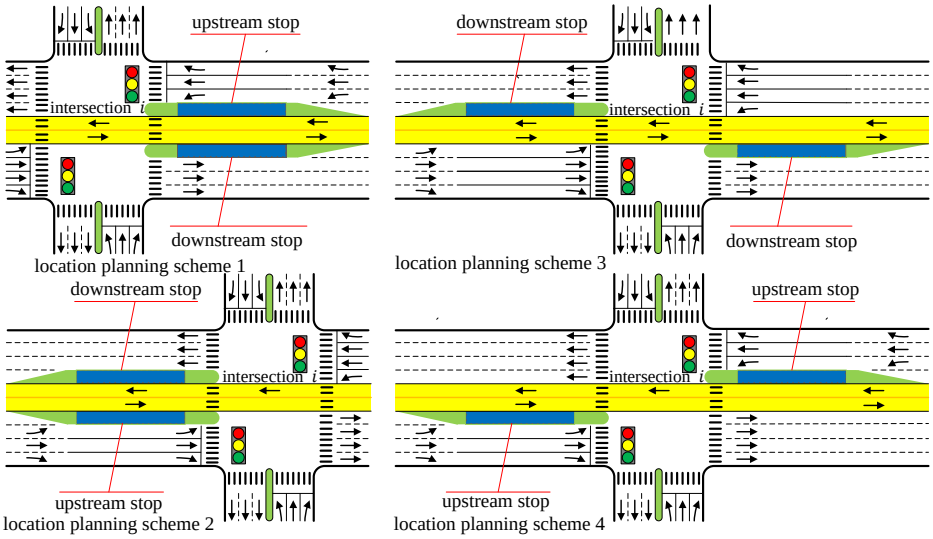

Figure 1. Location planning of BRT stops at a given intersection.

In this chapter, a Mixed Integer Nonlinear Programming (MINP) model is developed, which can accommodate cars and Bus Rapid Transit (BRT) simultaneously. Section 2.1 provides the definition of parameters and variables. Section 2.2 describes the decision variables of the model. Section 2.3 presents the objective function of the model that can guarantee the traffic efficiency of both cars and BRT vehicles. Section 2.4 includes some constraints and proposes a delay prediction model to formulate the signal delay of BRT vehicles at intersections.

2.1. Notations Description

The notations for parameters and variables used to facilitate the description of the proposed model are summarized in Table 1.

Table 1. Definition of parameters and variables.

Sets	Descriptions
I	The set of all intersections, $I = \{1, 2, \cdots, n\}$, where n denotes the number of intersections on the artery.
M_1	The set of all BRT vehicles in the outbound, $M_1 = \{1, 2, \cdots, N_1\}$, where N_1 denotes the number of BRT vehicles passing the outbound of the artery during the study period.
M_2	The set of all BRT vehicles in the inbound, $M_2 = \{1, 2, \cdots, N_2\}$, where N_2 denotes the number of BRT vehicles passing the inbound of the artery during the study period.
M	The set of all the two-way BRT vehicles, $M = \{M_1 \cup M_2\}$.
D	The set of the traveling directions, $D = \{1, 2\}$, where 1 denotes the outbound and 2 denotes the inbound.
Parameters	**Descriptions**
C	Public cycle length of intersections (s).
r_{id}	Red time of intersection i in coordinated direction d (s), $i \in I,\ d \in D$.
$L_{i-1,i,d}$	Intersection spacing, that is, the distance between intersection $i-1$ and intersection i in direction d (m), $i \in I,\ d \in D$.
v_{car}	Average speed of cars (m/s).
v_{bus}	Average speed of BRT (m/s).
σ_{id}	Dwelling time of BRT at intersection i in direction d (s), $i \in I,\ d \in D$.
$t_{i-1,i,d}$	Travel time of cars from intersection $i-1$ to intersection i in direction d (s), $i \in I,\ d \in D$.
α	The weight coefficient in green wave bandwidth of cars, $\alpha \in [0, 1]$.
τ_{md}	The entering time of the BRT vehicle m, which denotes the time that the vehicle enters the research area (s), $m \in M,\ d \in D$.
ρ	ρ is a weight coefficient in the objective function, $\rho \in [0, 1]$.
Variables	**Descriptions**
b_d	The green wave bandwidth of cars in direction d (s), $d \in D$.
B	Two-way total green wave bandwidth of cars (s).
Δt_{1d}	Total dwelling time at all stops of BRT on the road section from the starting point of the artery to the starting intersection (the first intersection) in direction d (s), $d \in D$.
$t_{i-1,i,d}$	Total dwelling time at all stops of BRT on the road section from intersection $i-1$ to intersection i in direction d (s), $i \in I,\ d \in D$.
$T_{i,m,d}$	Arrival time of BRT m at intersection i in direction d (s), $i \in I,\ m \in M,\ d \in D$.
$U_{i-1,i,d}$	Travel time of BRT from intersection $i-1$ to intersection i in direction d (s), $i \in I,\ d \in D$.
w_{id}	w_{i1} denotes the time interval from the left side of the green wave bandwidth of the car to the red light end time at the intersection i in the outbound, and w_{i2} denotes the time interval from the right side of the green wave bandwidth of the car to the red light start time at the intersection i in the inbound (s), $i \in I,\ d \in D$.
$\varphi_{i-1,i,d}$	$\varphi_{i-1,i,1}$ is the time interval from the intersection $i-1$ on the left side of the green wave bandwidth of cars to the red light start time at the intersection i in the outbound (s). $\varphi_{i-1,i,2}$ is the time interval from the intersection $i-1$ on the right side of the green wave bandwidth of cars to the red light end time at the intersection i in the inbound (s), $i \in I,\ d \in D$.
$O_{i-1,i,d}$	Relative offset of intersection i relative to intersection $i-1$ in direction d (s), $i \in I,\ d \in D$.
θ_{id}	Absolute offset of the intersection i in direction d (s), selecting the first intersection in direction d as the reference intersection, $i \in I,\ d \in D$.
δ_{id}	Location planning of BRT stops at the intersection i in direction d. δ_{id} is the binary variable, the value of "1" indicates that stop is arranged upstream of the intersection, and the value of "0" indicates that stop is arranged downstream of the intersection, $i \in I,\ d \in D$.
$D_{i,m,d}$	Signal delay of BRT m at intersection i in direction d (s), $i \in I,\ m \in M,\ d \in D$.
D_a	Average delay of BRT on the artery during the study period (s).

2.2. Decision Variables

The decision variables of the model are (i) the optimal locations of BRT stops at both directions on the artery (δ_{id}) and (ii) the offset between intersections on the artery (θ_{id}).

2.3. Objective Function

The objective function of the model is shown in Equation (1). D_a is the average BRT delay on the artery, equal to the total delay of all BRT vehicles at all intersections on the

artery divided by the number of BRT vehicles (as shown in Equation (2)). B is the two-way total green wave bandwidth of cars, as shown in Equation (3). ρ is the weight coefficient:

$$maximize\ ((1-\rho)B - \rho D_a) \tag{1}$$

$$D_a = \left(\sum_{d=1}^{2}\sum_{m=1}^{N}\sum_{i=1}^{n} D_{i,m,d}\right)/N, \quad (m \in M;\ d \in D;\ i \in I) \tag{2}$$

$$B = \sum_{d=1}^{2} b_d, \ \ (d \in D) \tag{3}$$

2.4. Problem Constraints

2.4.1. Offset Constraints

Considering the adjacent two intersections $i-1$ and i as an example, the travel time of cars from intersection $i-1$ to intersection i in direction d can be calculated as:

$$t_{i-1,i,d} = L_{i-1,i,d}/v_{car}, \quad (i = 2,3,\cdots,n;\ d \in D) \tag{4}$$

where v_{car} is the average speed of cars, and where $L_{i-1,i,d}$ is the distance between intersections $i-1$ and i in direction d.

The signal timing parameters of the arterial intersections and the green wave bandwidth diagram of cars are shown in Figure 2. In the diagram, point A is the red light start time of intersection $i-1$ in the outbound, point B is the green wave start time of intersection i in the outbound, point C is the green wave end time of intersection i in the inbound, and point D is the red light end time of intersection $i-1$ in the inbound. $\varphi_{i-1,i,1}$ is the time interval from intersection $i-1$ on the left side of the green wave bandwidth of cars to the red light start time at intersection i in the outbound, and $\varphi_{i-1,i,2}$ is the time interval from intersection $i-1$ on the right side of the green wave bandwidth of cars, to the red-light end time, at intersection i in the inbound. According to Figure 2, in the outbound, the time interval from point A to B can be represented by the left part of Equation (5). Similarly, in the inbound, the time interval from point C to D can be represented by the right part of Equation (5):

$$\varphi_{i-1,i,d} + r_{id} + w_{id} = r_{(i-1)d} + w_{(i-1)d} + t_{i-1,i,d}, \quad (i = 2,3,\cdots,n;\ d \in D) \tag{5}$$

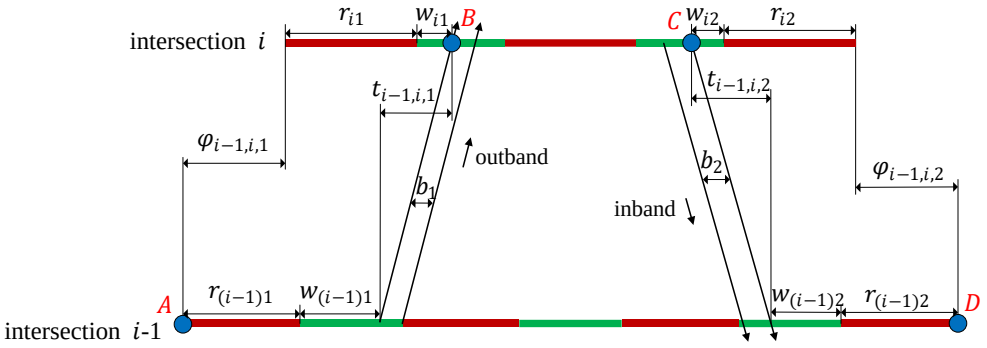

Figure 2. Signal timing and green−wave bandwidth.

The arterial signal coordination control scenario is shown in Figure 3, and the offset of intersections can be calculated using Equation (6). The sum of the offsets between any two adjacent intersections should be equal to the cycle time C, as shown in Equation (7):

$$O_{i-1,i,d} = C \times \left(\frac{\varphi_{i-1,i,d}}{C} - int\left[\frac{\varphi_{i-1,i,d}}{C}\right]\right), \quad (i = 2,3,\cdots,n;\ d \in D) \tag{6}$$

$$\sum_d O_{i-1,i,d} = C, \quad (i = 2,3,\cdots,n;\ d \in D) \tag{7}$$

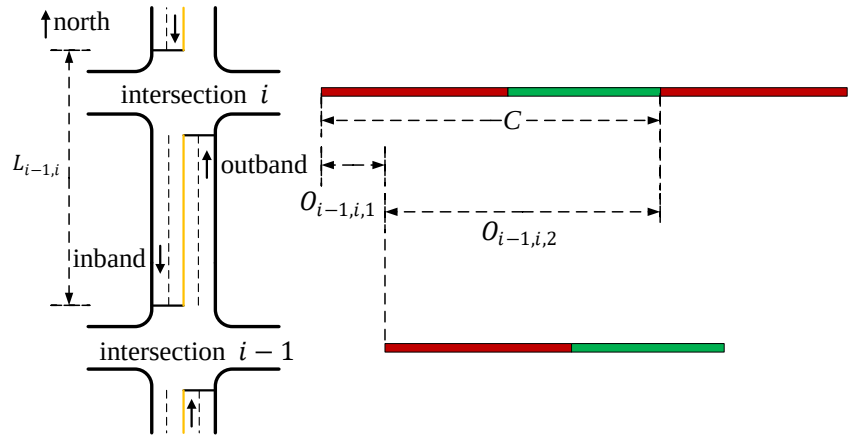

Figure 3. Coordinated signal control scenario.

2.4.2. Prediction of BRT Delays

(i) The delay characteristics of BRT

BRT vehicles pass through multiple intersections when driving along the artery. Whether the BRT will experience signal delay at an intersection mainly depends on the arrival time of the BRT vehicle at the intersection, as shown in Figure 4. However, the arrival time of the BRT vehicle is associated with the travel time, locations of the BRT stop, time spent by the BRT vehicle at stops (called the dwell time in the rest of the paper), and the signal delay of the BRT at the upstream intersection.

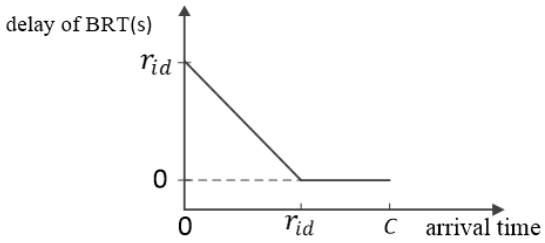

Figure 4. BRT delay.

In this section, we calculate the BRT's signal delay at intersections, considering the location planning of stops. The signal delay calculation method for the first intersection along the corridor (called starting intersection) is different from that of other intersections, and we consider this first below.

(ii) BRT delay at the starting intersection

In direction d, the BRT vehicles will stop once or will not stop when travelling to the starting intersection, and, therefore, the relationship between the dwell time of the BRT vehicles at the stop (Δt_{1d}) and the location planning of BRT (δ_{1d}) is shown in Equation (8):

$$\Delta t_{1d} = \delta_{1d} \times \sigma_{1d}, \quad (d \in D) \tag{8}$$

where δ_{1d} is the binary variable that represents the location planning of BRT stops at the starting intersection in direction d. $\delta_{1d} = 1$ indicates that the stop is arranged upstream of the intersection, $\delta_{1d} = 0$ indicates that the stop is arranged downstream of the intersection, and σ_{1d} represents the dwell time of the BRT vehicles at the first bus stop in direction d.

$T_{1,m,d}$ indicates that the arrival time of BRT m is at the starting intersection in direction d, as shown in Equation (9), which is equal to the sum of the entering time ($\tau_{m,d}$), dwell time at stops (Δt_{1d}), and the travel time ($L_{0,1,d}/v_{bus}$):

$$T_{1,m,d} = \tau_{m,d} + \Delta t_{1d} + L_{0,1,d}/v_{bus}, \quad (m \in M;\ d \in D) \tag{9}$$

We use Equation (9) to calculate the arrival time of the BRT vehicle at the starting intersection ($T_{1,m,d}$). The space–time trajectory of the BRT vehicle arriving at the starting intersection is shown in Figure 5. The signal delay of BRT m at intersection i in direction d can be expressed by Equation (10):

$$D_{1,m,d} = \begin{cases} C \times \left\{ \frac{r_{1d}}{C} - \left(\frac{T_{1,m,d}}{C} - int\left[\frac{T_{1,m,d}}{C} \right] \right) \right\}, & 0 \le \frac{T_{1,m,d}}{C} - int\left[\frac{T_{1,m,d}}{C} \right] < \frac{r_{1d}}{C} \\ 0, & \frac{r_{1d}}{C} \le \frac{T_{1,m,d}}{C} - int\left[\frac{T_{1,m,d}}{C} \right] < 1 \end{cases}, \quad (m \in M; d \in D) \tag{10}$$

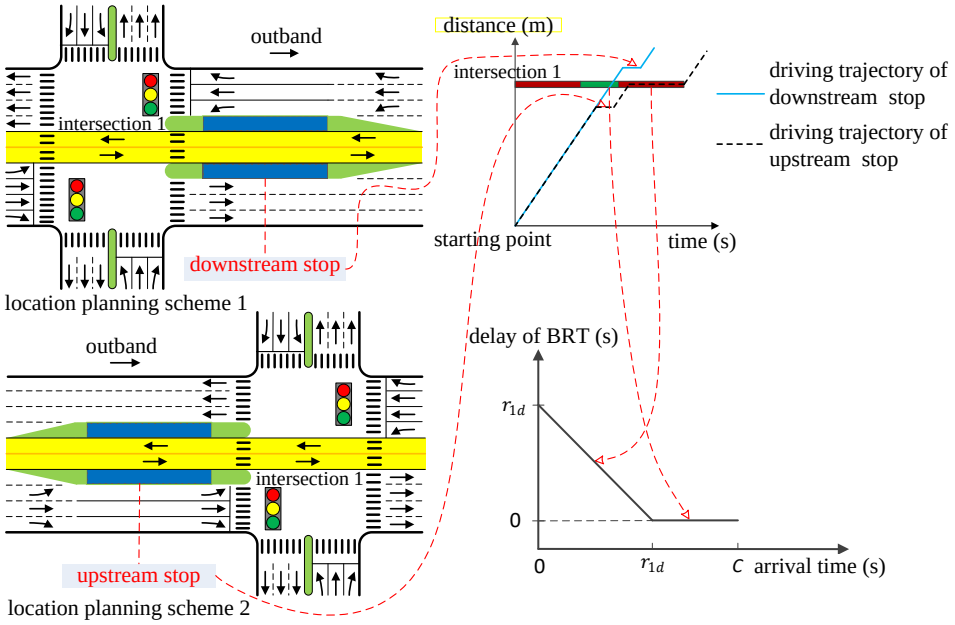

Figure 5. BRT delay at the starting intersection.

(iii) BRT delay at the other intersections

In direction d, there are four location-planning schemes of the BRT stops for any two adjacent intersections. Taking the outbound direction as an example, the location planning of BRT stops is shown in Figure 6. If the BRT stop is located at the upstream of the intersection, BRT vehicles can use the red light of the intersection to get passengers on and off, but they may also miss the green light due to the boarding and alighting process. If the BRT stop is located downstream of the intersection, the situation is just the opposite.

According to the location planning of stops and space–time trajectory in Figure 6, the BRT delay at intersection i is not only affected by the location planning of the stop of intersection i but also by stop location planning of upstream intersection $i-1$, which will also affect the arrival time of the BRT vehicle at intersection i, thus affecting the BRT delay at intersection i. In addition, the impact of the offset setting of the intersection on the signal delay of the BRT should be considered.

In direction d, for any two adjacent intersections, the BRT vehicles can only stop twice, and the relationship between the dwell time of the BRT vehicles at stops and the location planning of stops at intersections $i-1$ and i is shown in Equation (11):

$$\Delta t_{i-1,i,d} = \left(1 - \delta_{(i-1)d}\right) \times \sigma_{(i-1)d} + \delta_{id} \times \sigma_{id}, (i = 2, 3, \cdots, n;\ d \in D) \tag{11}$$

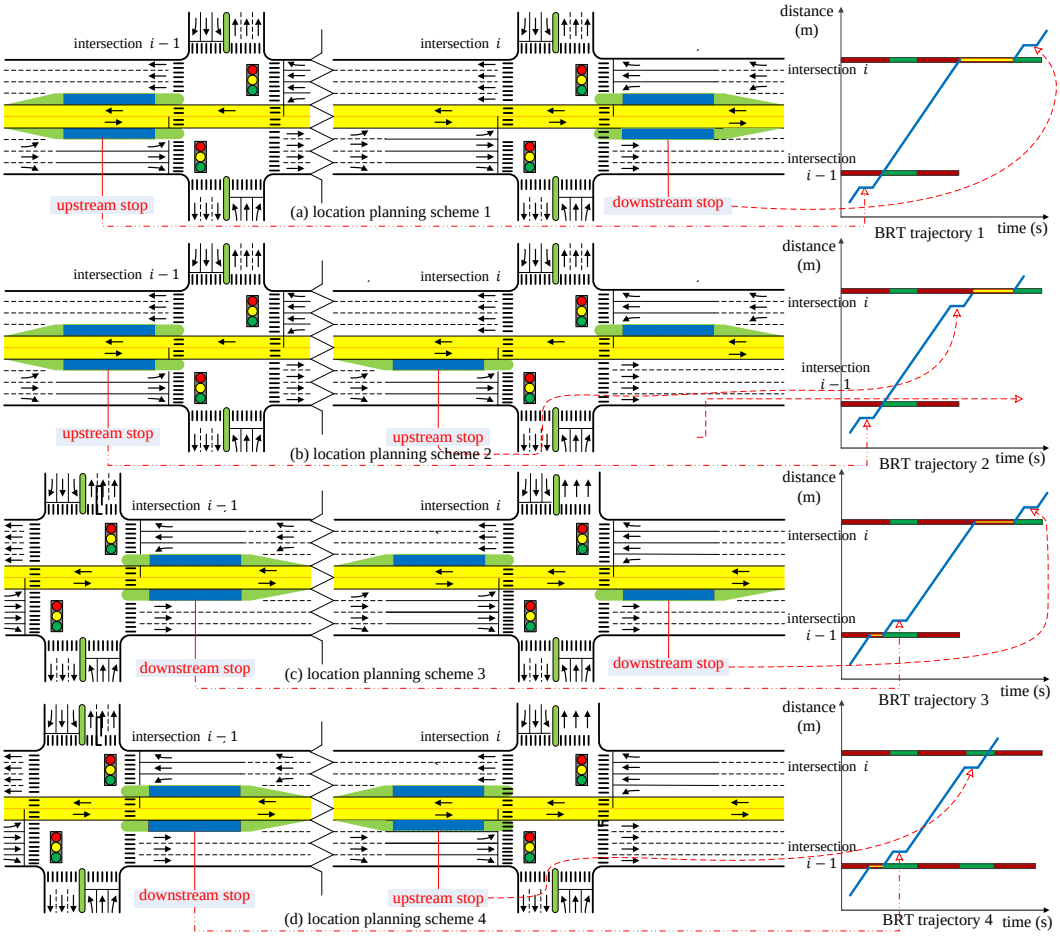

Figure 6. Location of stops and space–time trajectory of the BRT.

Equation (12) shows the travel time of the BRT vehicle from intersection $i-1$ to intersection i. $U_{i-1,i,d}$ is equal to the sum of the dwell time of the BRT vehicle at stops and the arterial travel time.

$$U_{i-1,i,d} = \Delta t_{i-1,i,d} + \frac{L_{i-1,i,d}}{v_{bus}}, \quad (i = 2,3,\cdots,n;\ d \in D) \tag{12}$$

Taking the starting intersection in direction d as the reference intersection, the absolute offset of intersection i in direction d can be expressed as:

$$\theta_{id} = \sum_{p=2}^{i} O_{p-1,p,d} - int\left[\frac{\sum_{p=2}^{i} O_{p-1,p,d}}{C}\right] * C, \quad (i = 2,3,\cdots,n;\ d \in D) \tag{13}$$

where $T_{i,m,d}$ is the arrival time of BRT m at intersection i in direction d, which is defined as:

$$T_{i,m,d} = T_{1,m,d} + \sum_i U_{i-1,i,d} + D_{1,m,d} + \sum_i D_{i-1,m,d} - \theta_{id}\ (i = 2,3,\cdots,n;\ m \in M;\ d \in D) \tag{14}$$

The signal delay of the BRT at the intersection depends on the arrival time point of the BRT vehicle in the signal cycle. As the BRT vehicle may arrive at the downstream intersection after multiple-signal cycles, the arrival cycle of the BRT vehicle is determined by the rounding down function $int[x]$. We use $\frac{T_{i,m,d}}{C} - int\left[\frac{T_{i,m,d}}{C}\right]$ to calculate the arrival time point of the BRT vehicle and the signal delay of the BRT at intersections. The signal delay ($D_{i,m,d}$) of BRT m at intersection i in direction d is calculated as follows:

Case 1: $D_{i,m,d}$ can be calculated using Equation (15), when the BRT vehicle arrives at the red time:

$$D_{i,m,d} = C \times \left\{ \frac{r_{id}}{C} - \left(\frac{T_{i,m,d}}{C} - int\left[\frac{T_{i,m,d}}{C} \right] \right) \right\}, \quad (i = 2, 3, \cdots, n;\ m \in M;\ d \in D) \tag{15}$$

Case 2: When the BRT vehicle arrives during the green time, $D_{i,m,d} = 0$.

2.4.3. Green Wave Bandwidth of Cars

The two-way green wave bandwidth of cars between any two adjacent intersections is shown in Figure 7. Using intersection i as an example in the outbound direction, the sum of the end of the red time at upstream intersection i to the left side of the green wave band of cars (w_{i1}) and green wave bandwidth of cars (b_1) should not be greater than the available green time. In other words, in the inbound direction, the sum of the time till the start of the red time at upstream intersection i (to the right side of the green wave band of cars, w_{i2}) and the green wave bandwidth of cars (b_2), should not be greater than the available green time. That is, Equation (16) should be satisfied:

$$w_{id} + b_d \le C - r_{id}, \quad (i \in I;\ d \in D) \tag{16}$$

where b_d is the green wave bandwidth of cars in direction d, C is the cycle time, and r_{id} is the red time of intersection i in direction d.

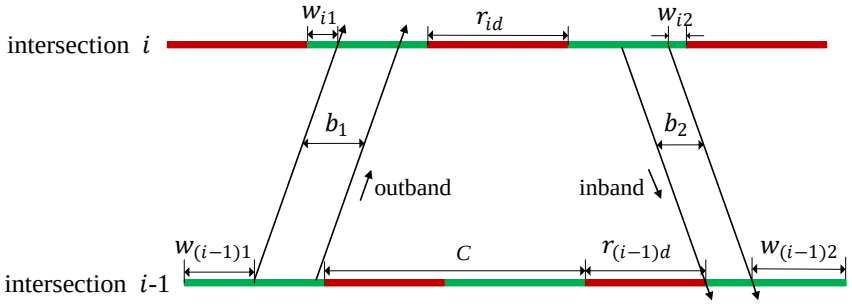

Figure 7. Two−way green wave bandwidth of cars between adjacent intersections.

b_d and w_{id} should be non-negative, satisfying Equations (17) and (18). B is the total green wave bandwidth of cars of the two directions. We use the weight coefficient α of the green wave bandwidth to adjust the green wave bandwidth of each direction:

$$b_d \ge \alpha \times B \ge 0, \quad (d \in D) \tag{17}$$

$$w_{id} \ge 0, \quad (i \in I;\ d \in D) \tag{18}$$

3. Solving the Model

The final model is formed as a mixed integer nonlinear programming (MINLP) problem, which is described as follows:

Decision variables: δ_{id}, θ_{id}.

Objective function: $maximize\ ((1-\rho)B - \rho D_a)$.

Constraints: Equations (4)–(18).

The nonlinear constraints of the model are of two main types: (i) the rounding function $int[x]$, as shown in Equations (6), (10), (13) and (15), and (ii) a piecewise function, as shown in Equation (10).

3.1. Linearization of the Rounding Function

Taking Equation (6) as an example, Equation (6) contains a nonlinear constraint, i.e., $int\left[\frac{\varphi_{i-1,i,d}}{C}\right]$, which makes it difficult for the model to obtain the optimal solution. We define an integer variable K_{id} as shown in Equations (19), and then we have:

$$K_{id} \in Z, \quad (i = 2, 3, \cdots, n;\ d \in D) \tag{19}$$

$$K_{id} \le \frac{\varphi_{i-1,i,d}}{C} - \varepsilon, \quad (i = 2, 3, \cdots, n;\ d \in D) \tag{20}$$

$$K_{id} \ge \frac{\varphi_{i-1,i,d}}{C} - 1, \quad (i = 2, 3, \cdots, n;\ d \in D) \tag{21}$$

where Z is the integer set.

Based on Equations (19)–(21), Equation (6) can be rewritten as the linear form, i.e.,

$$O_{i-1,i,d} = C \times \left(\frac{\varphi_{i-1,i,d}}{C} - K_{id}\right), \quad (i = 2, 3, \cdots, n;\ d \in D) \tag{22}$$

3.2. Linearization of the Piecewise Functions

Equation (10) contains a rounding function ($int\left[\frac{T_{1,m,d}}{C}\right]$), and Equation (10) is a piecewise function. We linearize the rounding function ($int\left[\frac{T_{1,m,d}}{C}\right]$) similar to Section 3.1, where we have:

$$k_{1,m,d} \in Z, \quad (m \in M;\ d \in D) \tag{23}$$

$$k_{1,m,d} \le \frac{T_{1,m,d}}{C} - \varepsilon, \quad (m \in M;\ d \in D) \tag{24}$$

$$k_{1,m,d} \ge \frac{T_{1,m,d}}{C} - 1, \quad (m \in M;\ d \in D) \tag{25}$$

$$\frac{T_{1,m,d}}{C} - int\left[\frac{T_{1,m,d}}{C}\right] = \frac{T_{1,m,d}}{C} - k_{1,m,d}, \quad (m \in M;\ d \in D) \tag{26}$$

In order to linearize the piecewise function, we define three continuous variables, i.e., $z^1_{1,m,d}$, $z^2_{1,m,d}$, $z^3_{1,m,d}$, and two binary variables, i.e., $y^1_{1,m,d}$, $y^2_{1,m,d}$, where we have:

$$\frac{T_{1,m,d}}{C} - k_{1,m,d} = 0 \times z^1_{1,m,d} + \frac{r_{1d}}{C} \times z^2_{1,m,d} + z^3_{1,m,d}, \quad (m \in M;\ d \in D) \tag{27}$$

$$z^1_{1,m,d} \le y^1_{1,m,d},\ \ z^2_{1,m,d} \le y^1_{1,m,d} + y^2_{1,m,d},\ \ z^3_{1,m,d} \le y^2_{1,m,d}, \quad (m \in M;\ d \in D) \tag{28}$$

$$\sum_{\beta=1}^{3} z^{\beta}_{1,m,d} = 1, \quad (m \in M;\ d \in D) \tag{29}$$

$$\sum_{\gamma=1}^{2} y^{\gamma}_{1,m,d} = 1, \quad (m \in M;\ d \in D) \tag{30}$$

$$D_{1,m,d}(0) = \frac{r_{1d}}{C},\ D_{1,m,d}\left(\frac{r_{1d}}{C}\right) = 0,\ \ D_{1,m,d}(1) = 0, \quad (m \in M;\ d \in D) \tag{31}$$

where $D_{1,m,d}(0)$ indicates the delay of BRT m at the starting intersection in direction d when the red light is turned on, $D_{1,m,d}\left(\frac{r_{1d}}{C}\right)$ indicates the delay of BRT m at the starting intersection in direction d when the signal light changes from red to green, $D_{1,m,d}(1)$ indicates the delay of BRT m at the starting intersection in direction d when the signal light turns red in the next cycle, $z^{\beta}_{1,m,d}$ ($z^1_{1,m,d}$, $z^2_{1,m,d}$, $z^3_{1,m,d}$) indicate the continuous variables, and $y^{\gamma}_{1,m,d}$ ($y^1_{1,m,d}$ and $y^2_{1,m,d}$) indicate the binary variables.

Based on Equations (23)–(31), Equation (10) can be rewritten as the linear form, i.e.,

$$D_{1,m,d} \times \left(\frac{T_{1,m,d}}{C} - m_{id} \right) = z^1_{1,m,d} \times D_{1,m,d}(0) + z^2_{1,m,d} \times D_{1,m,d}\left(\frac{r_{1d}}{C} \right) + z^3_{1,m,d} \times D_{1,m,d}(1), \quad (m \in M;\ d \in D) \tag{32}$$

After linearization, the MINLP problem is transformed into the standard mixed integer linear programming (MILP) problem. The model is programmed with AMPL (A Mathematical Programming Language) and solved efficiently with the Gurobi solver.

4. Case Study

4.1. Parameter Input

This case study considers an artery with a BRT line and six intersections in Jinan, Shandong region in eastern China. The artery starts from Beiyuan Street and runs to Jiefang Road, where Jinan BRT line 2 passes through the artery (Figure 8).

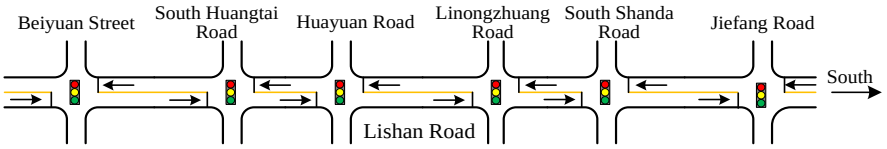

Figure 8. Schematic diagram of the research region.

The entering time timetable of the BRT during the morning peak, 7:00–8:00 a.m., is shown in Table 2.

Table 2. Entering time timetable.

Entering Order	**1**	**2**	**3**	**4**	**5**
Entering time	7:12	7:24	7:36	7:48	8:00

Other parameters are shown in Table 3, where, $\rho = 0.5$ is used in the objective function, and the sensitivity analysis will be conducted in the subsequent analysis.

Table 3. Parameter inputs.

Basic Parameters					
BRT speed v_{bus} (m/s)	Car speed v_{car} (m/s)	Cycle C (s)	Dwell time of BRT at stops σ_{id} (s)	Weight coefficient in objective function ρ	Weight Coefficient of Bandwidth α
11	15	150	26	0.5	0.45

Intersection spacing and signal timing parameters					
	Outbound		Inbound		
Intersections	Intersection spacing (m)	Red time (s)	Intersections	Intersection spacing (m)	Red time (s)
Beiyuan Street	220	95	Jiefang Road	220	90
Huangtai Road	671	75	South Shanda Road	698	91
Huayuan Road	354	103	Lilongzhuang Road	376	76
Lilongzhuang Road	698	76	Huayuan Road	698	103
South Shanda Road	376	91	Huangtai Road	354	75
Jiefang Road	698	90	Beiyuan Street	671	95

We program and solve the model in AMPL. There are 561 variables and 1326 constraints. The problem is solved with a Win 10 64-bit operating system, 11th Gen Intel® Core™ i5-11300H @ 3.10 GHz 2.61 GHz, 16 GB RAM. The average solving time is 8.03 s.

4.2. Comparison and Analysis

The scheme comparison is used to evaluate the performance of the proposed model. We compare and analyze the scheme proposed in this paper (optimizing the location

planning of BRT stops and the offset between intersections simultaneously) with the other seven schemes, which are described as follows:

Scheme 1: The current location planning of BRT stops and the current offset setting.

Scheme 2: The location planning of BRT stops is optimized and the current offset setting is used.

Scheme 3: The offset setting is optimized, and the current location planning of BRT stops is used.

Scheme 4: The BRT stops are located upstream of the intersections and the offset is not optimized.

Scheme 5: The BRT stops are located upstream of the intersections and the offset is optimized.

Scheme 6: The BRT stops are located downstream of the intersections and the offset is not optimized.

Scheme 7: The BRT stops are located downstream of the intersections and the offset is optimized.

4.2.1. Scheme Comparison

The location planning of BRT stops and the offset setting of intersections in the proposed and comparison schemes are shown in Table 4.

Table 4. Location planning of BRT stops and the offset of intersections.

Schemes	Direction	Location Planning of BRT Stops					
		Beiyuan Street	**Huangtai Road**	**Huayuan Road**	**Lilongzhuang Road**	**South Shanda Road**	**Jiefang Road**
Proposed scheme	Outbound	0	0	1	0	1	0
	Inbound	0	0	1	0	0	0
Scheme 1	Outbound	1	1	0	1	1	0
	Inbound	0	1	0	1	0	0
Scheme 2	Outbound	1	1	0	1	1	1
	Inbound	1	0	0	0	0	1
Scheme 3	Outbound	1	1	0	1	1	0
	Inbound	0	0	1	0	1	0
Scheme 4	Outbound	1	1	1	1	1	1
	Inbound	1	1	1	1	1	1
Scheme 5	Outbound	1	1	1	1	1	1
	Inbound	1	1	1	1	1	1
Scheme 6	Outbound	0	0	0	0	0	0
	Inbound	0	0	0	0	0	0
Scheme 7	Outbound	0	0	0	0	0	0
	Inbound	0	0	0	0	0	0
Schemes	**Direction**	**Offset of intersections (s)**					
		Beiyuan Street	**Huangtai Road**	**Huayuan Road**	**Lilongzhuang Road**	**South Shanda Road**	**Jiefang Road**
Proposed scheme	Outbound	0.00	97.54	58.18	145.73	10.82	74.27
	Inbound	75.73	23.27	133.91	71.45	86.55	0.00
Scheme 1	Outbound	0	44	66	78	14	114
	Inbound	36	80	102	114	50	0
Scheme 2	Outbound	0	44	66	78	14	114
	Inbound	36	80	102	114	50	0
Scheme 3	Outbound	0	75.2	75.2	136.8	15.6	90.1
	Inbound	59.9	135.1	135.1	46.7	75.5	0
Scheme 4	Outbound	0	44	66	78	14	114
	Inbound	36	80	102	114	50	0

Table 4. *Cont.*

Scheme 5	Outbound	0	91.9	51.8	139.4	14.1	68.7
	Inbound	81.3	23.3	133.1	70.6	95.4	0.0
Scheme 6	Outbound	0	44	66	78	14	114
	Inbound	36	80	102	114	50	0
Scheme 7	Outbound	0.0	91.0	50.9	139.4	6.2	67.8
	Inbound	82.2	23.3	133.1	71.6	88.5	0.0

Notes: In the table of location planning of BRT stops, 1 indicates that the stop is located upstream of the intersection, and 0 indicates that the stop is located downstream of the intersection.

4.2.2. Results Analysis

To compare the benefits of this proposed scheme with the other seven schemes, BRT delays and the green wave bandwidth of cars are selected as evaluation indexes.

(i) Analysis of BRT delays

The BRT delays under different schemes are shown in Table 5 and Figure 9.

Table 5. BRT delays under different schemes.

Schemes	Entering Time	Direction	Delay of BRT at the Intersections (s)							
			Beiyuan Street	Huangtai Road	Huayuan Road	Lilong-zhuang Road	South Shanda Road	Jiefang Road	Total One-Way Delay	Total Two-Way Delay
Proposed scheme	7:12	Outbound	0.0	0.0	0.0	0.0	0.0	0.0	0.0	0.0
		Inbound	0.0	0.0	0.0	0.0	0.0	0.0	0.0	
	7:24	Outbound	0.0	0.0	30.0	0.0	0.0	0.0	30.0	41.8
		Inbound	0.0	0.0	0.0	11.8	0.0	0.0	11.8	
	7:36	Outbound	15.0	0.0	45.0	0.0	0.0	0.0	60.0	101.8
		Inbound	0.0	0.0	0.0	30.5	1.3	10.0	41.8	
	7:48	Outbound	45.0	0.0	45.0	0.0	0.0	0.0	90.0	161.8
		Inbound	0.0	0.0	0.0	30.5	1.3	40.0	71.8	
	8:00	Outbound	75.0	0.0	45.0	0.0	0.0	0.0	120.0	221.8
		Inbound	0.0	0.0	0.0	30.5	1.3	70.0	101.8	
Scheme 1	7:12	Outbound	79.0	0.0	0.0	0.0	15.2	35.5	129.7	336.5
		Inbound	39.0	67.8	49.5	14.8	35.5	0.0	206.7	
	7:24	Outbound	0.0	46.0	17.8	19.5	40.8	35.5	159.7	396.5
		Inbound	39.0	67.8	49.5	14.8	65.5	0.0	236.7	
	7:36	Outbound	0.0	0.0	93.8	19.5	40.8	35.5	189.7	456.5
		Inbound	39.0	67.8	49.5	14.8	85.5	10.0	266.7	
	7:48	Outbound	19.0	0.0	0.0	0.0	15.2	35.5	69.7	366.5
		Inbound	39.0	67.8	49.5	14.8	85.5	40.0	296.7	
	8:00	Outbound	49.0	0.0	0.0	0.0	15.2	35.5	99.7	426.5
		Inbound	39.0	67.8	49.5	14.8	85.5	70.0	326.7	
Scheme 2	7:12	Outbound	79.0	0.0	0.0	0.0	15.2	9.5	103.7	284.4
		Inbound	13.0	41.8	51.9	0.0	0.0	74.0	180.7	
	7:24	Outbound	0.0	46.0	17.8	19.5	40.8	9.5	133.6	194.3
		Inbound	13.0	41.8	5.9	0.0	0.0	0.0	60.7	
	7:36	Outbound	0.0	0.0	93.8	19.5	40.8	9.5	163.6	254.3
		Inbound	13.0	41.8	35.9	0.0	0.0	0.0	90.7	
	7:48	Outbound	19.0	0.0	0.0	0.0	15.2	9.5	43.7	164.4
		Inbound	13.0	41.8	51.9	0.0	0.0	14.0	120.7	
	8:00	Outbound	49	0.0	0.0	0.0	15.2	9.5	73.7	224.5
		Inbound	13.0	41.8	51.9	0.0	0.0	44.0	150.7	
Scheme 3	7:12	Outbound	0.0	0.0	18.7	0.0	0.0	64.8	83.5	91.5
		Inbound	0.0	0.0	0.0	0.0	8.0	0.0	8.0	
	7:24	Outbound	0.0	0.0	48.7	0.0	0.0	64.8	113.5	151.5
		Inbound	0.0	0.0	0.0	38.0	0.0	0.0	38.0	
	7:36	Outbound	15.0	0.0	63.7	0.0	0.0	64.8	143.5	211.5
		Inbound	0.0	0.0	0.0	58.0	0.0	10.0	68.0	
	7:48	Outbound	45.0	0.0	63.7	0.0	0.0	64.8	173.5	271.5
		Inbound	0.0	0.0	0.0	58.0	0.0	40.0	98	
	8:00	Outbound	75.0	0.0	63.7	0.0	0.0	64.8	203.5	331.5
		Inbound	0.0	0.0	0.0	58.0	0.0	70.0	128	

Table 5. *Cont.*

Schemes	Entering Time	Direction	Delay of BRT at the Intersections (s)							
			Beiyuan Street	Huangtai Road	Huayuan Road	Lilong-zhuang Road	South Shanda Road	Jiefang Road	Total One-Way Delay	Total Two-Way Delay
Scheme 4	7:12	Outbound	79.0	0.0	78.8	45.5	40.8	9.5	253.7	434.5
		Inbound	39.0	41.8	25.9	0.0	0.0	74.0	180.7	
	7:24	Outbound	0.0	46.0	0.0	37.4	40.8	9.5	133.7	344.5
		Inbound	39.0	41.8	64.4	0.0	65.5	0.0	210.7	
	7:36	Outbound	0.0	0.0	67.8	45.5	40.8	9.5	163.7	254.5
		Inbound	39.0	41.8	9.9	0.0	0.0	0.0	90.7	
	7:48	Outbound	19.0	0.0	78.8	45.5	40.8	9.5	193.7	314.5
		Inbound	39.0	41.8	25.9	0.0	0.0	14.0	120.7	
	8:00	Outbound	49.0	0.0	78.8	45.5	40.8	9.5	223.7	374.5
		Inbound	39.0	41.8	25.9	0.0	0.0	44.0	150.7	
Scheme 5	7:12	Outbound	79.0	0.0	64.6	0.0	0.0	64.8	207.5	339.5
		Inbound	0.0	0.0	0.0	50.1	6.9	74.0	132.0	
	7:24	Outbound	0.0	0.0	23.6	0.0	0.0	64.8	87.5	99.5
		Inbound	0.0	0.0	0.0	12.0	0.0	0.0	12.0	
	7:36	Outbound	0.0	0.0	53.6	0.0	0.0	64.8	118.4	159.5
		Inbound	0.0	0.0	0.0	41.1	0.0	0.0	41.1	
	7:48	Outbound	19.0	0.0	64.6	0.0	0.0	64.8	148.4	219.4
		Inbound	0.0	0.0	0.0	50.1	6.9	14.0	71	
	8:00	Outbound	49.0	0.0	64.6	0.0	0.0	64.8	178.4	279.4
		Inbound	0.0	0.0	0.0	50.1	6.9	44.0	101.0	
Scheme 6	7:12	Outbound	0.0	42.0	0.0	37.4	40.8	9.5	129.7	336.5
		Inbound	39.0	41.8	64.4	0.0	61.5	0.0	206.7	
	7:24	Outbound	0.0	72.0	0.0	37.4	40.8	9.5	159.7	246.5
		Inbound	39.0	41.8	0.0	0.0	5.9	0.0	86.7	
	7:36	Outbound	15.0	0.0	78.8	45.5	40.8	9.5	189.7	306.5
		Inbound	39.0	41.8	25.9	0.0	0.0	10.0	116.7	
	7:48	Outbound	45.0	0.0	78.8	45.5	40.8	9.5	219.7	366.5
		Inbound	39.0	41.8	25.9	0.0	0.0	40.0	146.7	
	8:00	Outbound	75.0	0.0	78.8	45.5	40.8	9.5	249.7	426.5
		Inbound	39.0	41.8	25.9	0.0	0.0	70.0	176.7	
Scheme 7	7:12	Outbound	0.0	0.0	18.7	0.0	0.0	64.8	83.5	91.5
		Inbound	0.0	0.0	0.0	8.0	0.0	0.0	8.0	
	7:24	Outbound	0.0	0.0	48.7	0.0	0.0	64.8	113.5	151.5
		Inbound	0.0	0.0	0.0	38.0	0.0	0.0	38.0	
	7:36	Outbound	15.0	0.0	63.7	0.0	0.0	64.8	143.5	211.5
		Inbound	0.0	0.0	0.0	58.0	0.0	10.0	68.0	
	7:48	Outbound	45.0	0.0	63.7	0.0	0.0	64.8	173.5	271.5
		Inbound	0.0	0.0	0.0	58.0	0.0	40.0	98.0	
	8:00	Outbound	75.0	0.0	63.7	0.0	0.0	64.8	203.5	331.5
		Inbound	0.0	0.0	0.0	58.0	0.0	70.0	128	

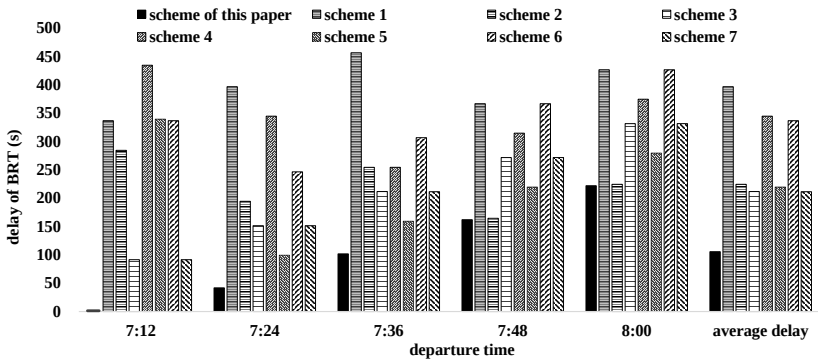

Figure 9. Comparison chart of BRT delays.

As shown in Table 5 and Figure 9, (A) under the "do not optimize the offset but the location planning of BRT stops" scheme, the BRT delay in scheme 2 was reduced by 43.4% compared with scheme 1. (B) When the location planning of BRT stops is similar, the

BRT delay can also be significantly reduced by optimizing the offset of each intersection on the artery. The scheme 3 delay is 46.7% lower than that of scheme 1, the scheme 5 delay is 36.3% lower than that of scheme 4, and the scheme 7 delay is 37.2% lower than that of scheme 6. (C) When the location planning of BRT stops and offset optimization is performed separately, the BRT delay is reduced to the same extent. The delay of scheme 3 (only optimizing the offset) is only 5.7% lower than that of scheme 2 (only optimizing the location planning of BRT stops), indicating that in reducing the BRT delay, the effect of optimizing the location planning of BRT stops on the artery is almost equivalent to that of optimizing the offset. (D) Optimizing the location planning of BRT stops and the offset between intersections simultaneously reduces the BRT delay significantly. Compared with the other seven schemes, the average BRT delay is reduced by 73.4%, 53.0%, 50.1%, 69.4%, 51.9%, 68.7%, and 50.1%, respectively. Figure 10 is the BRT vehicle trajectory and signal timing program.

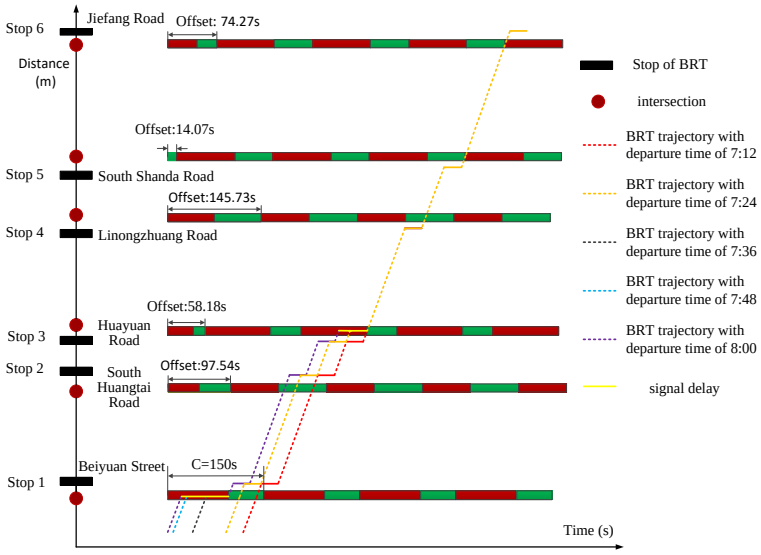

Figure 10. BRT trajectory and signal timing diagram.

(ii) Bandwidth analysis of cars

We analyzed the green wave bandwidth of cars. The continuous bandwidth of the six intersections of the proposed scheme and the other seven schemes is shown in Figure 11. When the offsets between intersections are not optimized, there is no green wave bandwidth of cars. In this study, the offsets are optimized to obtain the maximum two-way bandwidth of cars. Compared with the other seven schemes, the two-way bandwidth by use of the model described in this paper increases by 30.2% at a minimum, which is a very considerable traffic benefit for the cars and allows more cars to pass the intersections without stopping.

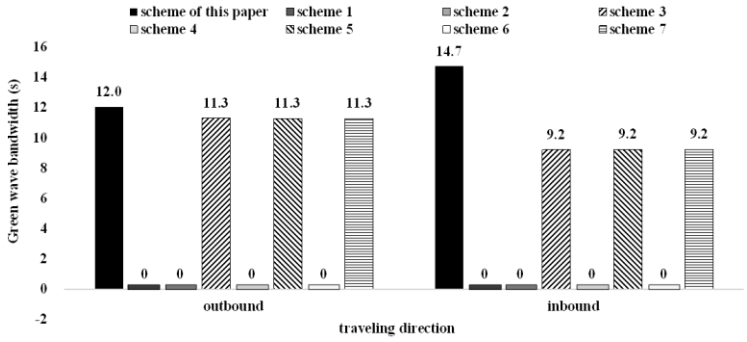

Figure 11. Comparison of the green−wave bandwidth of cars.

5. Sensitivity Analysis

5.1. Weight Coefficient

A sensitivity analysis of the weight coefficient in the objective function has been conducted. We change the value of ρ, and the values of other parameters remain the same, as in Section 5. The impact of ρ on the green wave bandwidth for cars is shown in Figure 12a; when ρ increases, the two−way bandwidth has a downward trend, and when $\rho \geq 0.6$, the bandwidth decreases rapidly to zero because the bandwidth between intersection 2 (South Huangtai Road) and intersection 3 (Huayuan Road) decreases to zero after the adjustment of the offset setting scheme. This can also be verified in Figure 13, where, when $\rho \geq 0.6$, the bandwidth rapidly decreases to zero.

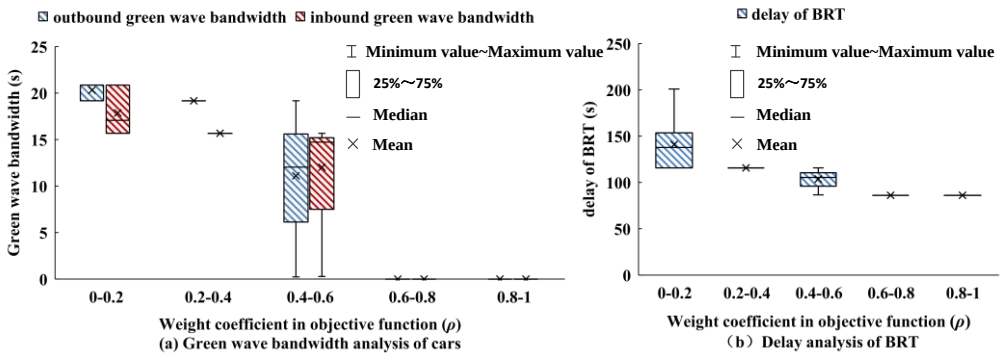

Figure 12. Sensitivity analysis of the weight coefficient in the objective function.

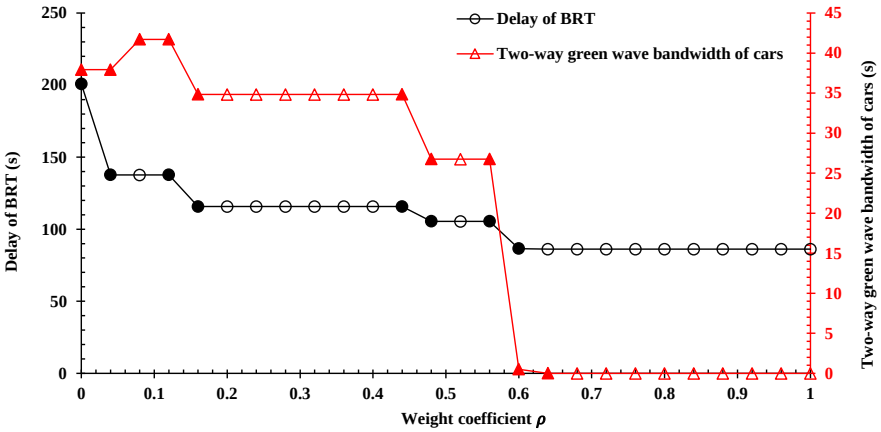

Figure 13. BRT delay (black) and green–wave bandwidth (red) of cars.

The impact of ρ on BRT delay is shown in Figures 12b and 13, where an increase in ρ causes the BRT delays on the artery to show, initially, a downward trend, but when $\rho \geq 0.6$, the BRT delays tend to be stable. This demonstrates that it is impossible to improve traffic efficiency of a BRT by sacrificing the bandwidth of cars.

5.2. BRT-Vehicle Speed

BRT vehicle speed is a key parameter in the delay prediction formula of the BRT, which can directly affect the arrival time of BRT vehicles at intersections. When analyzing the speed sensitivity of the BRT, only the value of the BRT speed is changed, while the other parameter settings are the same, as in Section 5. The average speed range of BRT vehicles on the artery is set to 9~14 $(\mathrm{m/s})$. The sensitivity analysis results of BRT vehicle speed are shown in Figure 14. In Figure 14a, the relationship between the average BRT vehicle speed and the bandwidth of cars is not obvious. The average bandwidth of cars shows a stable trend with the change in the average BRT speed. The influence of speed on BRT delay is shown in Figure 14b. When the average BRT speed increases, the BRT delay first decreases and then increases, indicating an obvious optimal value range. This result shows

the importance of optimizing speed in the field operation of BRT when considering the traffic control scheme in order to minimize the delay at the traffic lights.

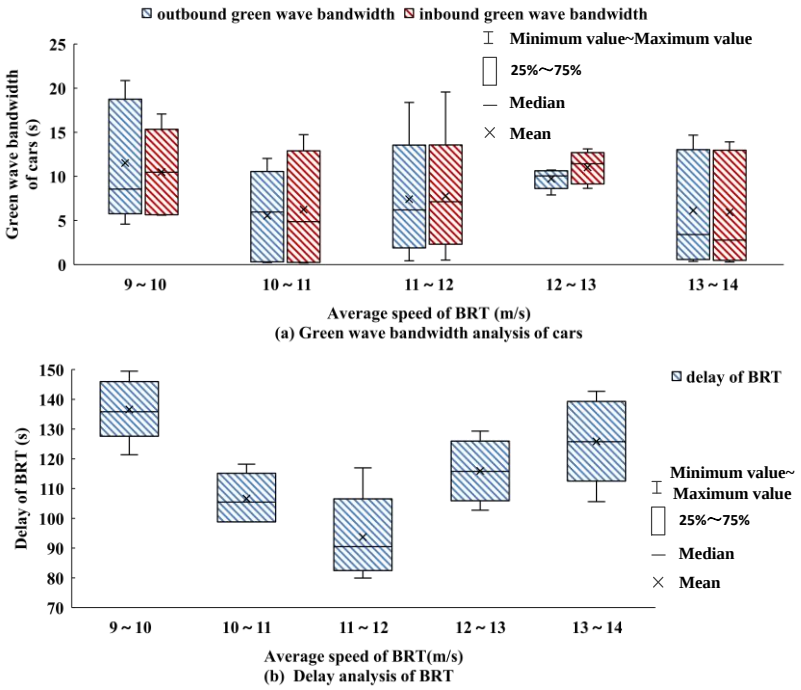

Figure 14. Sensitivity analysis of the BRT speed.

6. Conclusions

Existing signal coordination control models have mostly focused on the traffic flow of cars and tend to ignore or inefficiently deal with the traffic needs of public transit (e.g., BRT). BRT vehicles need to stop for passengers to get on and off at designated stops, increasing the travel time of BRT vehicles between intersections. Therefore, the signal coordination control strategies and their corresponding models that are developed primarily for the car traffic inevitably increase the signal delay of BRT systems, thus making it necessary to study a signal-timing model that also considers the BRT operation and is coordinated with the location planning of BRT stops.

In this study, we have considered and propose a new offset optimization model for signalized intersections that considers the traffic demand of BRT and cars simultaneously. The impact mechanism between setting BRT stops upstream or downstream of the intersections and the delay of BRT was analyzed, and the BRT delays at arterial intersections were predicted. Subsequently, considering the correlation between intersections, the location planning of BRT stops and the offset between intersections on the artery were optimized. A nonlinear combinatorial optimization model was established that takes the maximum weighted summation of BRT efficiency on the artery and green wave bandwidth of cars as the objective function, which takes the signal coordination control of intersections and the BRT-vehicle travel time as the constraints, and which optimizes the location planning of BRT stops and the offset between multi-intersections on the artery.

The proposed optimization method is compared with seven different alternative methods, and the results indicate that the proposed method can significantly reduce the signal delay of the BRT at intersections and provide maximum two-way bandwidth for cars. Moreover, the sensitivity analysis revealed that the optimization of the location planning of BRT stops has the same effect as the optimization of the offsets on the artery on reducing BRT delays, thus proving the importance of considering location planning of BRT stops when optimizing the offset between intersections on the artery.

The conclusion of the study is obtained based on the three assumptions mentioned in Section 1. However, we believe that the assumptions of the manuscript are reasonable. First,

similar to subways, the dwell time of BRT vehicles at bus stops is often fixed, and it can be obtained through field surveys. Second, the distance between two adjacent signalized intersection is generally around 400–800 m at the urban arterials in China. The bus stop is always located close to the intersection along the arterial to facilitate pedestrian crossing and transfer. Third, the fixed signal timing control is the most popular signal timing method utilized in the field because of its simplicity and low maintenance cost.

The proposed method can be extended in several ways. Firstly, this method can be extended from BRT to regular buses by considering the time-varying dwell-time at the bus stop. Secondly, bus stops and vehicles could affect dwell time and location due to poor service quality [35]. In future work, the impact of low service levels of bus stops and buses on dwell time can also be considered and evaluated. Bus stops and vehicles could affect dwell time and location due to poor service quality [35]. In future work, the impact of low service levels of bus stops and buses on dwell time can also be considered and evaluated. Furthermore, the proposed method can also to be evaluated with larger-sized problem instances in future studies. Finally, future studies can evaluate the proposed model in a multi-objective mode by considering more evaluation indexes, e.g., energy consumption, average travel cost, etc.

Author Contributions: Conceptualization, W.W., X.L. and B.S.; formal analysis, W.W., X.L. and B.S.; funding acquisition, W.W. and X.L.; investigation, X.L.; methodology, X.L.; validation, W.W. and X.L.; writing—original draft, X.L.; writing—review and editing, W.W. and B.S. All authors have read and agreed to the published version of the manuscript.

Funding: This study is supported by three fundings, which are Ministry of Education Humanities and Social Sciences Research Project (22YJCZH189), Changsha science and technology plan project funding (kq2107009), and Postgraduate Scientific Research Innovation Project of Hunan Province (CX20220868).

Data Availability Statement: Not unavailable.

Conflicts of Interest: The authors declare no conflict of interest.

References

1. Cao, M.; Yang, C. Research on Consumer Identity in Using Sustainable Mobility as a Service System in a Commuting Scenario. *Systems* **2022**, *10*, 223. [CrossRef]
2. Sun, Y.D.; Jiang, J.Y.; Lam, S.K.; He, P.L. Learning traffic network embeddings for predicting congestion propagation. *IEEE Trans. Intell. Transp. Syst.* **2022**, *23*, 11591–11604. [CrossRef]
3. Wu, W.; Ma, W.; Long, K.; Wang, Y. Integrated Optimization of Bus Priority Operations in Connected Vehicle Environment. *J. Adv. Transp.* **2016**, *50*, 1573–2337. [CrossRef]
4. Mylonakou, M.; Chassiakos, A.; Karatzas, S.; Liappi, G. System Dynamics Analysis of the Relationship between Urban Transportation and Overall Citizen Satisfaction: A Case Study of Patras City, Greece. *Systems* **2023**, *11*, 112. [CrossRef]
5. Li, M.; Boriboonsomsin, K.; Wu, G.Y.; Zhang, W.B. Traffic energy and emission reductions at signalized intersections: A study of the benefits of advanced driver information. *Int. J. Intell. Transp. Syst. Res.* **2009**, *7*, 2327–2332.
6. Schrank, D.; Albert, L.; Eisele, B.; Lomax, T. *2021 Urban Mobility Report*; The Texas A&M Transportation Institute: Bryan, TX, USA; INRIX: Kirkland, WA, USA, 2021.
7. Chen, J.X.; Wang, S.A.; Liu, Z.Y.; Chen, X.W. Network-level optimization of bus stop placement in urban areas. *KSCE J. Civ. Eng.* **2018**, *22*, 1446–1453. [CrossRef]
8. Wu, W.; Larry, H.; Yan, S.H.Y.; Ma, W.J. Development and evaluation of bus lanes with intermittent and dynamic priority in connected vehicle environment. *J. Intell. Transp. Syst.* **2018**, *22*, 301–310. [CrossRef]
9. AlRukaibi, F.; AlKheder, S. Optimization of bus stop stations in Kuwait. *Sustain. Cities Soc.* **2019**, *44*, 726–738. [CrossRef]
10. Cvitanic, D. Joint impact of bus stop location and configuration on intersection performance. *Promet-Traffic Transp.* **2017**, *29*, 443–454. [CrossRef]
11. Diab, E.I.; EI-Geneidy, A.M. The farside story measuring the benefits of bus stop location on transit performance. *Transp. Res. Rec.* **2015**, *2538*, 1–10. [CrossRef]
12. Cui, Y.; Chen, S.K.; Liu, J.F.; Jia, W.Z. Optimal locations of bus stops connecting subways near urban intersections. *Math. Probl. Eng.* **2015**, *2015*, 1563–5147. [CrossRef]
13. Furth, P.G.; SanClemente, J.L. Near Side, Far Side, Uphill, Downhill: Impact of Bus Stop Location on Bus Delay. *Transp. Res. Rec. J. Transp. Res. Board* **2006**, *1971*, 66–73. [CrossRef]

14. Tirachini, A. The economics and engineering of bus stops: Spacing, design and congestion. *Transp. Res. Part A Policy Pract.* **2014**, *59*, 37–57. [CrossRef]
15. Medina, M.; Giesen, R.; Muñoz, J.C. Model for the optimal location of bus stops and its application to a public transport corridor in Santiago, Chile. *Transp. Res. Rec. J. Transp. Res. Board* **2013**, *2352*, 84–93. [CrossRef]
16. Shatnawi, N.; Al-Omari, A.A.; Al-Qudah, H. Optimization of bus stops locations using GIS techniques and artificial intelligence. *Procedia Manuf.* **2020**, *44*, 52–59. [CrossRef]
17. Ziari, H.; Keymanesh, M.R.; Khabiri, M.M. Locating stations of public transportation vehicles for improving transit accessibility. *Transport* **2007**, *22*, 99–104. [CrossRef]
18. Carrizosa, E.; Harbering, J.; Schöbel, A. Minimizing the passengers' traveling time in the stop location problem. *J. Oper. Res. Soc.* **2016**, *67*, 1325–1337. [CrossRef]
19. Chien, S.I.; Qin, Z.Q. Optimization of bus stop locations for improving transit accessibility. *Transp. Plan. Technol.* **2004**, *27*, 221–227. [CrossRef]
20. Cheng, G.; Zhao, S.Z.; Zhao, T. A Bi-Level programming model for optimal bus stop spacing of a bus rapid transit system. *Mathematics* **2019**, *7*, 625. [CrossRef]
21. Ibeas, A.; dell'Olio, L.; Alonso, B.; Olivia, S. Optimizing bus stop spacing in urban areas. *Transp. Res. Part E Logist. Transp. Rev.* **2010**, *46*, 446–458. [CrossRef]
22. van de Weg, G.S.; Vu, H.L.; Hegyi, A.; Hoogendoorn, S.P. A Hierarchical Control Framework for Coordination of Intersection Signal Timings in All Traffic Regimes. *IEEE Trans. Intell. Transp. Syst.* **2019**, *20*, 1815–1827. [CrossRef]
23. Kim, E.S.; Wu, C.J.; Horowitz, R.; Arcak, M. Offset optimization of signalized intersections via, the Burer-onteiro method. In Proceedings of the 2017 American Control Conference (ACC), Seattle, WA, USA, 24–26 May 2017; pp. 3554–3559.
24. Zheng, L.; Feng, M.; Yang, X.; Xue, X.F. Stochastic simulation-based optimization method for arterial traffic signal coordination with equity and efficiency consideration. *IET Intell. Transp. Syst.* **2023**, *17*, 373–385. [CrossRef]
25. Ma, W.J.; An, K.; Lo, H.K. Multi-stage stochastic program to optimize signal timings under coordinated adaptive control. *Transp. Res. Part C Emerg. Technol.* **2016**, *72*, 342–359. [CrossRef]
26. Morgan, J.T.; Little, J.D.C. Synchronizing traffic signals for maximal bandwidth. *Oper. Res.* **1964**, *12*, 896–912. [CrossRef]
27. Ye, B.L.; Wu, W.M.; Mao, W.J. A two-way arterial signal coordination method with queueing process considered. *IEEE Trans. Intell. Transp. Syst.* **2015**, *16*, 3440–3452. [CrossRef]
28. Zhang, L.H.; Song, Z.Q.; Tang, X.J.; Wang, D.H. Signal coordination models for long arterials and grid networks. *Transp. Res. Part C Emerg. Technol.* **2016**, *71*, 215–230. [CrossRef]
29. Zhao, C.; Xie, Y.C.; Gartner, N.H.; Stamatiadis, C.; Arsava, T. Am-band: An asymmetrical multi-band model for arterial traffic signal coordination. *Transp. Res. Part C Emerg. Technol.* **2015**, *58*, 515–531.
30. Coogan, S.; Kim, E.; Gomes, G.; Arcak, M.; Varaiya, P. Offset optimization in signalized traffic networks via semidefinite relaxation. *Transp. Res. Part B Methodol.* **2017**, *100*, 82–92. [CrossRef]
31. Ouyang, Y.; Zhang, R.Y.; Lavaei, J.; Varaiya, P. Conic approximation with provable guarantee for traffic signal offset optimization. In Proceedings of the 2018 IEEE Conference on Decision and Control (CDC), Miami, FL, USA, 17–19 December 2018; pp. 229–236.
32. Ouyang, Y.; Zhang, R.Y.; Lavaei, J.; Varaiya, P. Large-scale traffic signal offset optimization. *IEEE Trans. Control Netw. Syst.* **2020**, *7*, 1176–1187. [CrossRef]
33. Wang, D.H.; Shen, X.Y.; Luo, X.Q.; Jin, S. Offset optimization with minimum average vehicle delay. *J. Jilin Univ. (Eng. Technol. Ed.)* **2021**, *51*, 511–523.
34. Barabino, B.; Bonera, M.; Ventura, R.; Maternini, G. Collective road transport infrastructural characteristics and spaces in the urban road regulation. Caratteristiche infrastrutturali e spazi del trasporto collettivo su gomma nel regolamento viario urbano. *Ing. Ferrov.* **2020**, *75*, 727–767.
35. Barabino, B. Automatic recognition of "low-quality" vehicles and bus stops in bus services. *Public Transp.* **2018**, *10*, 257–289. [CrossRef]